ELSEVIER

Journal of Magnetism and Magnetic Materials 161 (1996) L1–L5

Journal of magnetism and magnetic materials

Letter to the Editor

Exchange-spring behavior in sputter-deposited α-Fe/Nd–Fe–B multilayer magnets

M. Shindo [a,*], M. Ishizone [a], H. Kato [a], T. Miyazaki [a], A. Sakuma [b]

[a] *Department of Applied Physics, Faculty of Engineering, Tohoku University, Sendai 980-77, Japan*
[b] *Magnetic and Electronic Materials Research Laboratory, Hitachi Metals, Ltd., 5200 Mikajiri Kumagaya 360, Japan*

Received 5 June 1996; revised 2 August 1996

Abstract

Thin films of Nd–Fe–B and α-Fe/Nd–Fe–B multilayer with Ti both for underlayers and overlayers were fabricated on glass substrates by means of RF sputtering. After annealing at 873–973 K for 30 min, both Nd–Fe–B films and α-Fe/Nd–Fe–B multilayer films have shown relatively large coercive fields and the minor loops of the α-Fe/Nd-Fe-B multilayer films are reversible in a certain range of demagnetization fields. These results indicate that the layers of α-Fe and $Nd_2Fe_{14}B$ phases are exchange coupled.

PACS: 75.50.Ww; 75.70.-i; 81.15.Cd

Keywords: Nanocomposite magnet; $Nd_2Fe_{14}B$; α-Fe; Thin film; Exchange-coupling

1. Introduction

As electronic devices become small-sized, higher performance magnets have been required. Many studies have been making progress to obtain a larger maximum energy product beyond that of $Nd_2Fe_{14}B$ magnets. Recently, 'nanocomposite magnets' or 'exchange-spring magnets' [1] have been proposed to have a huge energy product far beyond that of $Nd_2Fe_{14}B$ magnets theoretically [2].

Nanocomposite magnets are fabricated mainly by means of melt-spinning or rapid-quenching process [3–6]. First getting amorphous flakes, they are subsequently annealed to get a nano-crystal structure containing hard and soft grains. At present, however, the maximum energy product have been much lower than those expected theoretically. The primary reason is thought to be a great gap between actual and ideal nanostructures (suitable size of the grains, good alignment of hard phases and so on). This gap is caused by the difficulty in controlling nanostructures in rapid-quenching processes. In order to approach to the ideal nanostructures and investigate exchange-coupled nanocomposite magnets systematically, we have introduced a thin-film technology, which is relatively easy to control nano-size structures. In this paper, we report the magnetic properties of Nd–Fe–B thin films and α-Fe/Nd–Fe–B multilayers with Ti both for underlayers and overlayers fabricated by means of RF sputtering.

* Corresponding author. Fax: +81-22-217-7947; email: shindo@mlab.apph.tohoku.ac.jp.

PII S0304-8853(96)00458-1

2. Experimental procedures

Thin films of Nd–Fe–B and α-Fe/Nd–Fe–B multilayers with Ti both for underlayers and overlayers were prepared with RF diode magnetron sputtering using $Nd_{13}Fe_{70}B_{17}$ alloy and 99.9% Fe metal targets with base pressure below 4.0×10^{-4} Pa. The sputtering gas was Ar at a pressure of 8.0×10^{-1} Pa. The α-Fe/Nd–Fe–B multilayer films have the form Ti/Fe/(Nd–Fe–B/Fe) × 5/Ti/glass, with the thickness of two Ti layers $d_{Ti} = 30$ nm, Fe layers varied between $d_{Fe} = 0$–30 nm, and Nd–Fe–B layers fixed at $d_{Nd-Fe-B} = 30$ nm. All the films were annealed at 873–973 K for 30 min with the pressure below 4.0×10^{-4} Pa to crystallize $Nd_2Fe_{14}B$ phase. The magnetization curves were measured by means of a vibrating sample magnetometer (VSM) with a maximum applied field of 15 kOe parallel to the film plane, and X-ray diffractometer (Fe K_α) was used to identify the phases present. The composition of Nd–Fe–B films were determined with EPMA and the distribution of the composition along the direction of the film thickness in α-Fe/Nd–Fe–B multilayer films were measured by means of Auger electron spectrometer.

3. Results and discussion

According to the EPMA experiments, the composition of the as-sputtered Nd–Fe–B films were found to be $Nd_{13-15}Fe_{bal}B_{7-11}$, so the films are expected to be almost of single phase containing $Nd_2Fe_{14}B$ grains. When the Nd–Fe–B films have been fabricated directly on the glass substrates without Ti underlayers and overlayers, the demagnetization curves after annealing at 973 K for 30 min exhibit a form of two independent magnetic phases as shown in Fig. 1. From X-ray diffraction, a large α-Fe (110) peak was observed in addition to the $Nd_2Fe_{14}B$ peaks. It is inferred that owing to the oxidization of Nd upon annealing, the quantity of remaining metallic Nd is too poor to keep a single phase containing $Nd_2Fe_{14}B$ grains. On the other hand, in the case of the films with Ti both for underlayers and overlayers, the magnetization curves have simple hysteresis

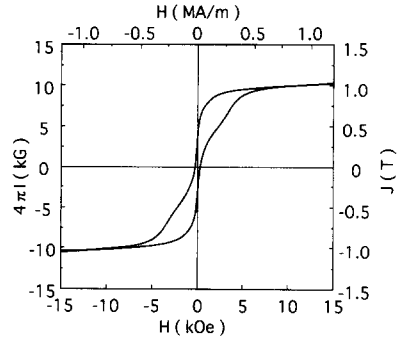

Fig. 1. Magnetization curve for Nd–Fe–B (1.0 μm)/glass at room temperature.

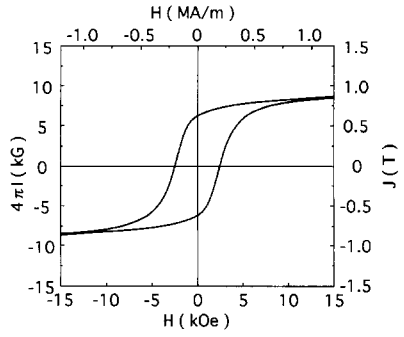

Fig. 2. Magnetization curve for Ti (0.1 μm)/Nd–Fe–B (1.0 μm)/Ti (0.1 μm)/glass at room temperature.

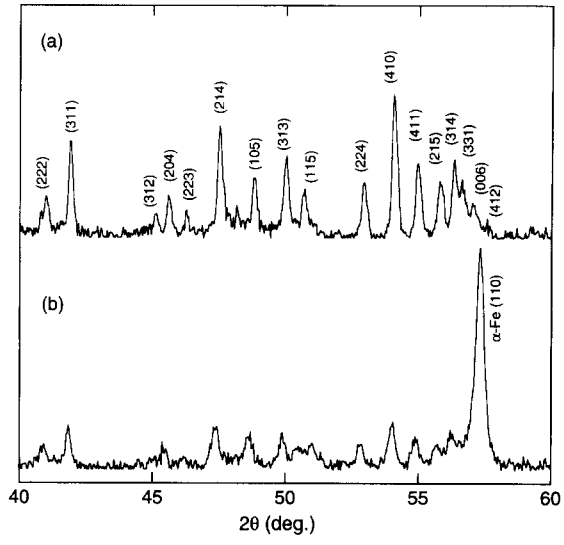

Fig. 3. X-ray diffraction pattern obtained by using the Fe K_α radiation: (a) Ti (0.1 μm)/Nd–Fe–B (1.0 μm)/Ti (0.1 μm)/glass, (b) Ti (30 nm)/Fe (50 nm)/[Nd–Fe–B (100 nm)/Fe (50 nm)]×5/Ti (30 nm)/glass.

loops of single hard phase. An example for Ti(0.1 μm)/Nd–Fe–B(1.0 μm)/Ti(0.1 μm)/glass is shown in Fig. 2. Almost all the X-ray diffraction peaks of these films were confirmed to be those of randomly oriented $Nd_2Fe_{14}B$ phase as shown in Fig. 3a. These results show that Ti sandwich layers are highly effective for preventing the Nd–Fe–B films from oxidation.

In the case of α-Fe/Nd–Fe–B multilayer films, we have also confirmed that Ti both for underlayers and overlayers can keep the films unoxidized upon annealing. The multilayer films having the form Ti(30 nm)/Fe(d_{Fe})/[Nd–Fe–B(30 nm)/Fe(d_{Fe})]×5/Ti(30 nm)/glass with d_{Fe} between 0 to 30 nm were fabricated and annealed at 873 K for 30 min. Figs. 4 and 5 show typical demagnetization curves of the obtained films, with $d_{Fe} = 5$ nm and 30 nm, respectively. Although the major loop in the former case approximately exhibits a form of single hard phase, minor loop behaviors are completely different. Namely, minor loops are reversible in a field range where the magnetization is relatively large. On the other hand, the major loop of the $d_{Fe} = 30$ nm sample resembles a form of two independent magnetic phases with reduced coercive field values. Minor loops are, however, almost reversible even if the demagnetization field value exceeds the coercive field, and the recoil permeability is quite high. Kneller and Hawig [1] have pointed out that, when the soft phase thickness is comparable to the domain wall thickness of the hard phase, the demagnetization curve resembles that of hard single phase but with

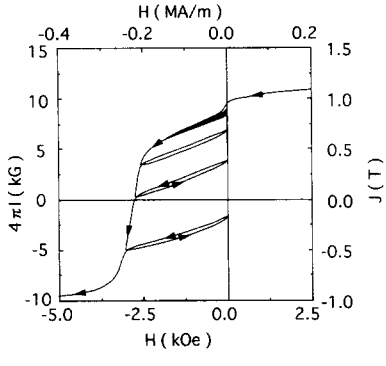

Fig. 4. Demagnetization curve for Ti (30 nm)/Fe (5 nm)/[Nd–Fe–B (30 nm)/Fe (5 nm)]×5/Ti (30 nm)/glass at room temperature.

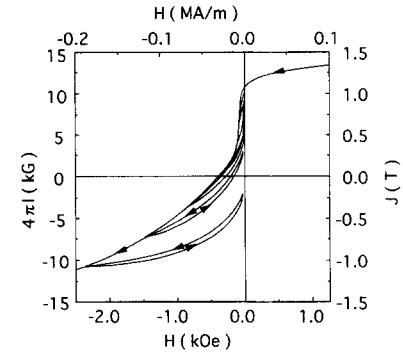

Fig. 5. Demagnetization curve for Ti (30 nm)/Fe (30 nm)/[Nd–Fe–B (30 nm)/Fe (30 nm)]×5/Ti (30 nm)/glass at room temperature.

the certain reversible range, in which the boundary between the reversible and irreversible regions depends on the volume fraction of the hard phase. In the case of large soft phase thickness, they have estimated that the reversible region extends over the coercive field as shown in Fig. 3b of Ref. [1]. Demagnetization curves of the present multilayer films given in Figs. 4 and 5 show the characteristic properties expected in nanocomposite magnets in small and large soft phase thickness, respectively, predicted by Kneller and Hawig [1]. Thus, these results strongly suggest that α-Fe and $Nd_2Fe_{14}B$ phases are exchange coupled in these multilayer films.

Fig. 6 shows the dependence of magnetization $4\pi I$ at the external field of $H = 15$ kOe, remanence B_r and coercivity ${}_iH_c$ on the thickness of the α-Fe d_{Fe} with fixed Nd–Fe–B phase thickness ($d_{Nd-Fe-B} = 30$ nm). All the samples were annealed at 873 K for 30 min. In Fig. 6a, we can see that $4\pi I$ increases with increasing d_{Fe}. We have calculated the $4\pi I$ as a function of d_{Fe} using the formula $4\pi I = 4\pi I_{Fe}V_{Fe} + 4\pi I_{Nd-Fe-B}V_{Nd-Fe-B}$, where V_{Fe}, $V_{Nd-Fe-B}$ ($= 1 - V_{Fe}$), $4\pi I_{Fe}$ and $4\pi I_{Nd-Fe-B}$ are the volume fractions and the magnetizations of α-Fe and Nd–Fe–B phases, respectively. The results of least-squares fitting, with $4\pi I_{Fe}$ and $4\pi I_{Nd-Fe-B}$ as adjustable parameters, are indicated by the solid line in Fig. 6a. The values of obtained parameters are $4\pi I_{Fe} = 19.5$ kG and $4\pi I_{Nd-Fe-B} = 11.3$ kG, which are in good agreement with experimental values of single phase

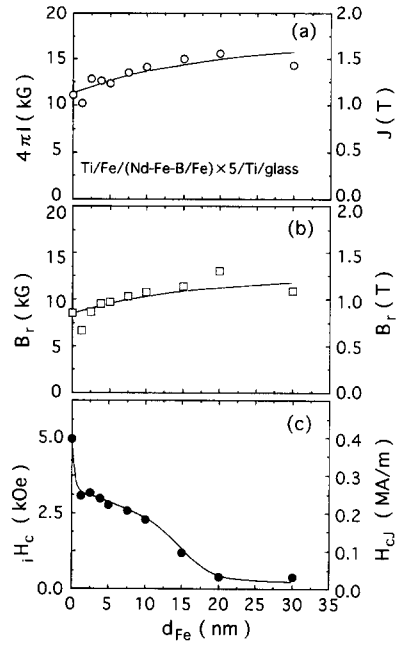

Fig. 6. (a) Magnetization $4\pi I$ at $H = 15$ kOe, (b) remanence B_r and (c) coercive field ${}_iH_c$ plotted as a function of α-Fe thickness d_{Fe} in α-Fe/Nd–Fe–B multilayer films. Solid line in (a) represents the result of fitting as described in the text, and the line in (b) is obtained by multiplying the line in (a) by 0.75, while the line in (c) is a guide to the eye.

films of α-Fe (18 kG) and Nd–Fe–B (11 kG), respectively. Thus, the dependence of $4\pi I$ on d_{Fe} has been confirmed to reflect the volume fraction of α-Fe and Nd–Fe–B phases. Al-Omari and Sellmyer [7] have recently reported the similar results for CoSm/FeCo bilayer films.

In Fig. 6b, we can see that B_r increases with increasing d_{Fe} as well as $4\pi I$, and the values of B_r are relatively large in spite of the random alignment of $Nd_2Fe_{14}B$ grains. The solid line shown in Fig. 6b is obtained by simply multiplying the fitting curve in Fig. 6a by 0.75, which is in relatively good agreement with the experimental values of B_r. Thus, the films have remanence enhancement $B_r/4\pi I$ of about 0.75, which is approximately independent of d_{Fe}. It is inferred that large values of B_r arise from the presence of α-Fe phase and also from the remanence enhancement induced by the exchange coupling.

As shown in Fig. 6c, ${}_iH_c$ decreases with increasing d_{Fe} and the rate of decrease becomes significant for $d_{Fe} > 10$ nm. This behavior is approximately consistent with the theoretical prediction by Kneller and Hawig [1] and the computer simulations by Skomski and Coey [2], in which ${}_iH_c$ begins to decrease when the soft phase thickness exceeds the domain-wall thickness of hard phase.

We have made the X-ray diffraction experiments on these multilayer films. However, for the series of Ti(30 nm)/Fe(d_{Fe})/[Nd–Fe–B(30 nm)/Fe(d_{Fe})] × 5/Ti(30 nm)/glass, it was impossible to detect diffraction peaks of $Nd_2Fe_{14}B$ owing probably to the smallness of total thickness of the $Nd_2Fe_{14}B$ phase and the sensitivity limit of the diffractometer. As for the thicker samples we did observe the distinct peaks as shown, for example, in Fig. 3b for Ti(30 nm)/Fe(50 nm)/[Nd–Fe–B(100 nm)/Fe(50 nm)] × 5/Ti(30 nm)/glass. Since the dependence of magnetic properties on d_{Fe} in the Ti(30 nm)/Fe(d_{Fe})/[Nd–Fe–B(100 nm)/Fe(d_{Fe})] × 5/Ti(30 nm)/glass series has been found to be similar to that of Ti(30 nm)/Fe(d_{Fe})/[Nd–Fe–B(30 nm)/Fe(d_{Fe})] × 5/Ti(30 nm)/glass series, we expect that the $Nd_2Fe_{14}B$ crystal phase is stabilized even in the latter thin multilayers.

In order to directly check the multilayer structure in the annealed sample, Auger electron spectroscopy experiments have been performed along the direction of film thickness in Ti/Fe/(Nd–Fe–B/Fe) × 5/Ti/glass multilayers. Clear stepwise-like change in Fe concentration was observed as well as changes in Nd and B concentrations with opposite phase to that of Fe. In samples for d_{Fe}, $d_{Nd-Fe-B} < 10$ nm, however, significant diffusion of Nd and B has been noticed, although the periodic changes of concentrations still exist corresponding to the designed thickness. The interface width obtained by the Auger experiments are about 10 nm, which would be larger than the actual width, since the effect of interface roughness would be convoluted into the depth profile data.

We are now performing a computer simulation of the magnetization curves in order to analyze the present results. Preliminary results have shown that we can at least qualitatively reproduce the different behaviors observed in small and large d_{Fe} samples with the fixed interlayer exchange-coupling strength which is set to be about an order of magnitude smaller than that of the intralayer couplings. It should be noted, however, that not all the atoms at the

interface of hard and soft phases might be exchange coupled. By combining the present experiments and simulation, we can at least infer that the effective coupling strength between soft and hard phases, which is the product of the coupling constant per pair at the interface and the number of the coupled pair, is not greatly affected by the soft phase thickness. Detailed results of the simulation, including the dependence of coercive fields and energy product on the Fe layer thickness will be published elsewhere.

4. Conclusions

Films of the form Ti/Nd–Fe–B/Ti/glass and Ti/Fe/[Nd–Fe–B/Fe] × 5/Ti/glass have been prepared by RF sputtering. We have obtained the following conclusions. (1) Ti both for underlayers and overlayers prevent the magnetic phases from oxidization upon annealing. (2) In the α-Fe/Nd–Fe–B multilayer films, $4\pi I$ increases with increasing d_{Fe}, which are in accordance with a simple estimation based upon the superposition of magnetization of α-Fe and Nd–Fe–B phases. (3) The coercive field ${}_{i}H_{c}$ in the α-Fe/Nd–Fe–B multilayer films decreases with increasing d_{Fe}, which is approximately consistent with the theoretical prediction [1] and calculation [2]. (4) The minor loops of the α-Fe/Nd–Fe–B multilayer films have exhibited a spring-back behavior, in which different behaviors observed in small and large d_{Fe} samples clearly corresponds to those predicted by Kneller and Hawig [1]. (5) The α-Fe/Nd–Fe–B multilayer films thus have all the characteristic magnetic properties expected in nanocomposite magnets, which have proved that α-Fe and $Nd_2Fe_{14}B$ phases are exchange coupled in these multilayer films.

References

[1] E.F. Kneller and R. Hawig, IEEE Trans. Magn. 27 (1991) 3588.
[2] R. Skomski and J.M.D. Coey, Phys. Rev. B48 (1993) 812.
[3] L. Withwanawasam, A.S. Murphy, G.C. Hadjipanayis and R.F. Krause, J. Appl. Phys. 76 (1994) 7065.
[4] R. Coehoorn, D.B. de Mooij, J.P.W. Duchateau and K.H.J. Buschow, J. Phys. (Paris) C8 (1988) 669.
[5] R. Coehoorn, D.B. de Mooij and C. de Waard, J. Magn. Magn. Mater. 80 (1989) 101.
[6] S. Hirosawa, H. Kanekiyo and M. Uehara, J. Appl. Phys. 73 (1993) 6488.
[7] I.A. Al-Omari and D.J. Sellmyer, Phys. Rev. B 52 (1995) 3441.